The Evidence for Fullerene Aggregation in High-Performance Small-Molecule Solar Cells by Molecular Dynamics Simulation

Guankui Long, Ailin Li, Rui Shi, Ye-Cheng Zhou, Xuan Yang, Yi Zuo, Wei-Ru Wu, U-Ser Jeng, Yanting Wang, Xianjian Wan, Panwen Shen, Hao-Li Zhang, Tianying Yan, and Yongsheng Chen**

Solution-processed small-molecule-based organic photovoltaics (SM-OPVs) have recently stimulated more and more research interests, owing to its well-defined structures, less batch to batch variation, more easily controlled energy levels and absorption, etc.,[1–5] compared with polymer OPVs (P-OPVs). The power conversion efficiency (PCE) of SM-OPVs has recently reached over 10%,[6–8] and it is expected to eventually approach or even exceed polymer solar cells.[9,10] Our group has reported a series of acceptor–donor–acceptor (A–D–A)-type oligothiophene derivatives[4] which exhibit very promising performance for solution-processed SM-OPV devices,[11–13] and PCEs over 9% have recently been achieved by using 2,2′-((5Z,5′Z)-5,5′-((3,3′′′′,3′′′′′,3′′′′′′,4′,4″-hexaoctyl-[2,2′:5′,2″:5″,2′′′:5′′′,2′′′′:5′′′′,2′′′′′:5′′′′′,2′′′′′′-sepithiophene]-5,5′′′′′′-diyl)bis(methanylylidene))bis(3-ethyl-4-oxothiazolidine-5,2-diylidene))dimalononitrile (**DRCN7T**) as the donor material.[7] **Scheme 1** shows the chemical structures of **DRCN7T** and (5Z,5′Z)-5,5′-((3,3′′′′,3′′′′′,3′′′′′′,4′,4″-hexaoctyl-[2,2′:5′,2″:5″,2′′′:5′′′,2′′′′:5′′′′,2′′′′′:5′′′′′,2′′′′′′-sepithiophene]-5,5′′′′′′-diyl)bis(methanylylidene))bis(3-ethyl-2-thioxothiazolidin-4-one) (**DERHD7T**), respectively. With the introduction of dicyanomethylene (DCM) groups to replace the thio groups in **DERHD7T**,[14] the morphology has been significantly changed from large phase-separated domains (30–70 nm) for **DERHD7T** blended with [6,6]-phenyl-C$_{71}$-butyric acid methyl ester (PC$_{71}$BM) to highly crystalline fibrillar-type (diameters of ≈10 nm) morphology[15,16] for **DRCN7T**:PC$_{71}$BM, and the power conversion efficiency has also been increased dramatically from 4.35% to 9.30% for the OPV devices.[7] In order to further investigate the origin of the efficient charge separation and the structure–performance relationship from the molecular level for these oligothiophene derivatives, we employed the molecular dynamic (MD) simulations to study the micromorphology[17–26] of these two representative small-molecule-based OPV systems in this work.

We speculated that the introduction of the DCM groups could increase the ground state dipole moment and enhance the intermolecular interactions between neighboring oligothiophene molecules. Meanwhile, these strong interactions between **DRCN7T** molecules would weaken the intermolecular interactions with PC$_{71}$BM, thus could provide a suitable environment for the aggregation of the PC$_{71}$BM through the solvophobic assembly.[27] On the other hand, recent studies have confirmed the importance of fullerene aggregation, which is proved to be the key driver for efficient charge separation in OPV.[28,29] Based on the time-resolved ultrafast pump–probe results, Friend et al.[30] found that relatively ordered domains of fullerenes at the donor:acceptor interfaces could allow the electrons to access the delocalized "band-like" states, which would lead to the ultrafast and efficient charge separation through delocalized band-like states in these fullerene aggregates.[31–33] Ratner and co-workers[34] also demonstrated that the fullerene cluster size, concentration, and dimensionality would have large impact on the charge generation efficiency through theoretical calculations. On the basis of those results, in this work,

---

Dr. G. Long, X. Yang, Y. Zuo, Dr. X. Wan, Prof. Y. Chen
Key Laboratory of Functional Polymer Materials
Collaborative Innovation Center of Chemical
Science and Engineering (Tianjin)
Center for Nanoscale Science and Technology
Institute of Polymer Chemistry
College of Chemistry
Nankai University
Tianjin 300071, China
E-mail: yschen99@nankai.edu.cn

Dr. A. Li, Prof. P. Shen, Prof. T. Yan
Institute of New Energy Material Chemistry
Tianjin Key Laboratory of Metal- and
Molecule-Based Material Chemistry
Collaborative Innovation Center of
Chemical Science and Engineering (Tianjin)
College of Chemistry
Nankai University
Tianjin 300071, China
E-mail: tyan@nankai.edu.cn

Dr. R. Shi, Prof. Y. Wang
State Key Laboratory of Theoretical Physics
Institute of Theoretical Physics
Chinese Academy of Sciences
Beijing 100190, China

Y.-C. Zhou, Prof. H.-L. Zhang
State Key Laboratory of Applied Organic Chemistry (SKLAOC)
College of Chemistry and Chemical Engineering
Lanzhou University
Lanzhou 730000, China

Dr. W.-R. Wu, Prof. U.-S. Jeng
National Synchrotron Radiation Research Center
Hsinchu Science Park, Hsinchu 30077, Taiwan

Dr. W.-R. Wu, Prof. U.-S. Jeng
Chemical Engineering Department
National Tsing-Hua University
Hsinchu 30013, Taiwan

DOI: 10.1002/aelm.201500217

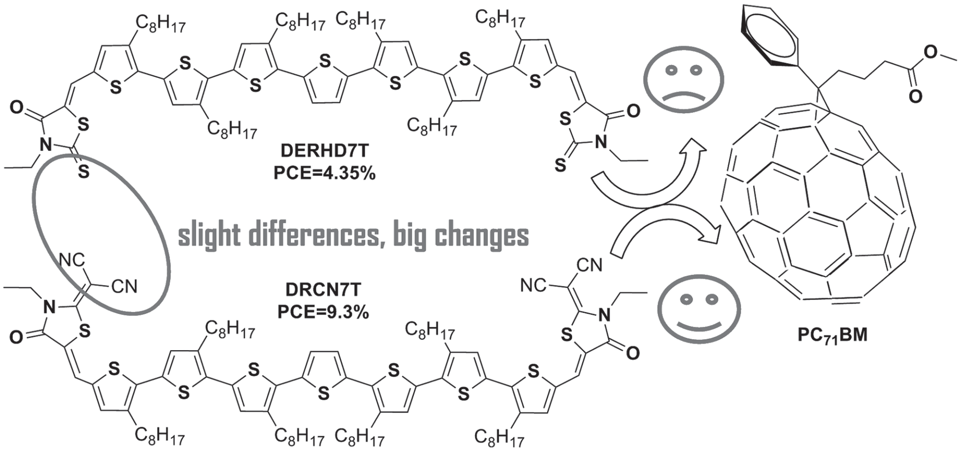

Scheme 1. Chemical structures of **DERHD7T**, **DRCN7T**, and $PC_{71}BM$.

we focused on investigating the molecular origin of fullerene aggregation at the donor:acceptor interfaces by MD simulation. We have found that, with the introduction of the DCM groups, the acceptor molecules exhibit a stronger aggregation, and the DCM groups also exhibit very regular interaction with $PC_{71}BM$, which facilitates the electron delocalization during the charge separation process,[35] and thus contributes to the efficient charge separations in the bulk-heterojunction (BHJ) blends.

The MD simulations were carried out using the GROMACS program (version 4.5.5),[36–38] and the detailed information about the simulations could be found in the Experimental Section (Figures S1 and S2, Tables S1–S10, Supporting Information). In order to benchmark the simulation model, we have compared the simulated X-ray diffraction (XRD)[39,40] with the experimental powder-XRD for **DERHD7T**:$PC_{71}BM$ and **DRCN7T**:$PC_{71}BM$ blends, and the simulated XRD profiles match reasonably well with the experimental results (Figure S3, Supporting Information). Then the snapshots of the simulated unit cells for **DERHD7T**:$PC_{71}BM$ and **DRCN7T**:$PC_{71}BM$ are shown in **Figure 1**a,b, respectively, **DERHD7T** and fullerene acceptors are well mixed, while the $PC_{71}BM$ molecules aggregate tighter in **DRCN7T**:$PC_{71}BM$ than in **DERHD7T**:$PC_{71}BM$.

The stronger intermolecular interactions between **DRCN7T** molecules than **DERHD7T** in the blends with $PC_{71}BM$ could be proved by investigating the radial distribution function (RDF) of the rhodanine groups in the oligothiophene donors. The rhodanine groups are the high-polarized groups in the oligothiophene backbones, which were influenced by the different electron-withdrawing ability of thio groups (in **DERHD7T**) or dicyanomethylene groups (in **DRCN7T**). As shown in **Figure 2**a, the peak at ≈4.4 Å is the distance between intermolecular rhodanine groups, and the stronger and sharper peak in **DRCN7T**:$PC_{71}BM$ blends than **DERHD7T**:$PC_{71}BM$ further evident the stronger intermolecular interactions between **DRCN7T** molecules. The stronger intermolecular interactions between **DRCN7T** molecules than that of **DERHD7T** will lead to the weaker interactions between **DRCN7T** and $PC_{71}BM$. In order to further confirm this, the RDF between thiophene units in the oligothiophene donors and center-of-mass (COM) of C_{70} is calculated (Figure 2b). The thiophene units in **DERHD7T** have closer and compact contact with fullerene acceptors than that for **DRCN7T**. Meanwhile, the RDF between each thiophene units in the oligothiophene backbone and COM of C_{70} is also calculated and summarized in Figure S4 (Supporting Information). All these further evident the stronger interactions exist between **DRCN7T** molecules, which have weaken the intermolecular interactions with $PC_{71}BM$, and thus provided a more suitable environment for the aggregation of the $PC_{71}BM$ through the solvophobic assembly.

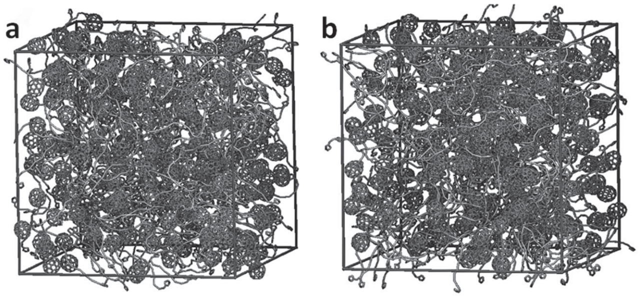

Figure 1. Snapshots of the unit cells of two representative small-molecule-based systems, a) **DERHD7T**:$PC_{71}BM$ and b) **DRCN7T**:$PC_{71}BM$ from the MD simulation. The alkyl groups on the oligothiophene derivatives and $PC_{71}BM$ are not shown for clarity. All the fullerene molecules are colored with cyan, and the oligothiophene donors were simplified to a ribbon with rhodanine end groups.

The packing modes for $PC_{71}BM$ in the two BHJ blends were depicted by the COM RDFs, as shown in **Figure 3**a. In both systems, three distinctive peaks indicate quite ordered structures of fullerenes. Especially, the first peak at ≈11 Å shows that in the **DRCN7T**-based system, the $PC_{71}BM$ molecules have a stronger aggregation within a short range. The higher RDF peak further confirmed that the $PC_{71}BM$ molecules packed more tightly in the mixture with **DRCN7T** than **DERHD7T**.

In order to experimentally confirm the stronger aggregation of fullerenes in the **DRCN7T**:$PC_{71}BM$ blends than the **DERHD7T**:$PC_{71}BM$ observed in our MD simulations, the 2D grazing incidence small-angle X-ray scattering (2D-GISAXS) was performed on the BHJ blends at Shanghai Synchrotron Radiation Facility (SSRF). The 2D scattering patterns for fullerene aggregation were collected on a charge coupled device camera, and the curve intensities versus *q* were obtained

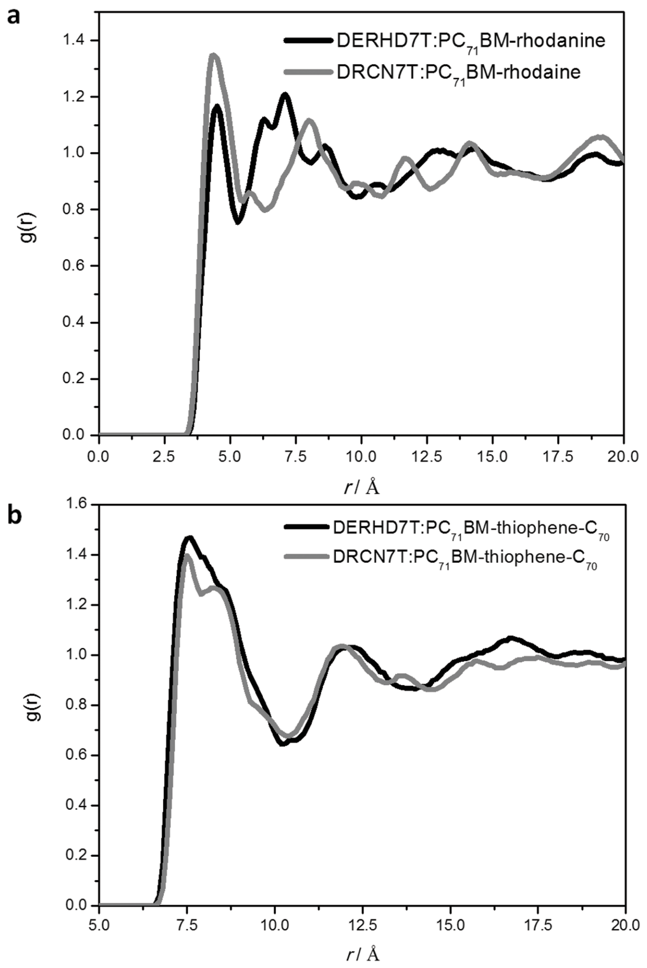

Figure 2. a) The RDF $g(r)$ for COM of rhodanine units of **DERHD7T**:PC$_{71}$BM (black line) and **DRCN7T**:PC$_{71}$BM (red line) blends. b) The RDF $g(r)$ for COM of thiophene units and C$_{70}$ of **DERHD7T**:PC$_{71}$BM (black line) and **DRCN7T**:PC$_{71}$BM (red line) blends.

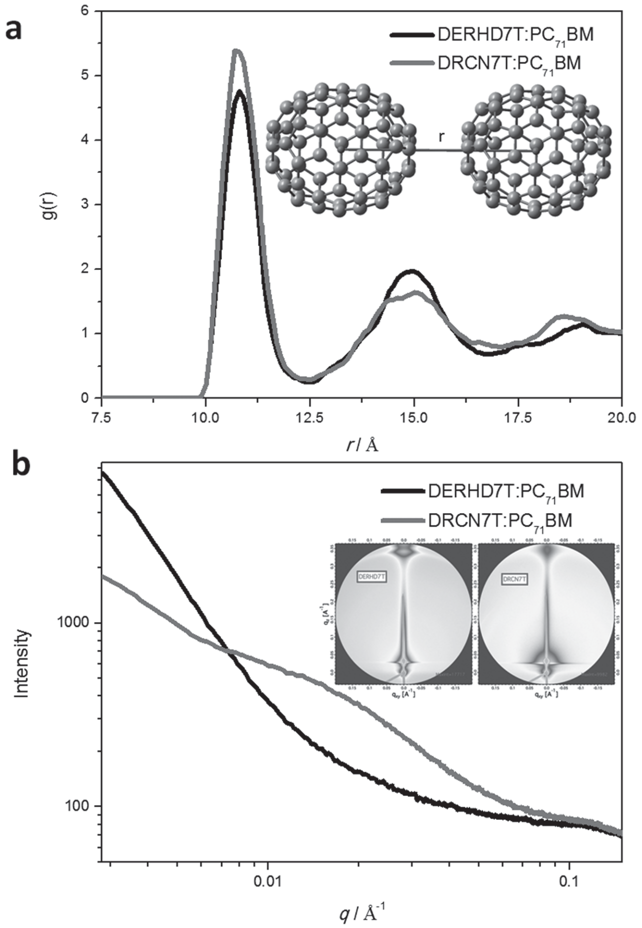

Figure 3. a) The COM of C$_{70}$ RDF $g(r)$ for **DERHD7T**:PC$_{71}$BM (black line) and **DRCN7T**:PC$_{71}$BM (red line) blends. b) GISAXS profiles measured for the **DRCN7T**:PC$_{71}$BM and **DERHD7T**:PC$_{71}$BM blends after post-thermal annealing at 100 °C for 10 min. The inset shows the 2D-GISAXS patterns for both blend films for comparison.

by integrating the data from the patterns, which is shown in Figure 3b. There exhibits a broad peak at q of 0.007–0.04 Å^{-1} in the **DRCN7T**:PC$_{71}$BM blend, which has been proved to reflect the scattering of fullerene aggregated domains.[41,42] Using polydisperse spheres model with the Schultz size distributions functions,[43] we obtained the fullerene domain size in **DRCN7T**:PC$_{71}$BM blend is 6.88 ± 0.51 nm, which is shown in Figure S5 (Supporting Information). In contrast, the **DERHD7T**:PC$_{71}$BM film did not show any obvious peaks in the 2D-GISAXS pattern and almost the same with the 2D-GISAXS pattern for pure **DERHD7T** film (Figure S6, Supporting Information), which indicates less fullerene aggregations in this BHJ blend. This is consistent with our simulation results that the **DRCN7T**-based system has a stronger fullerene aggregation which could facilitate both the exciton delocalization and charge separation at the donor:acceptor interfaces.

The next question is how the donor molecules interact with PC$_{71}$BM during the charge transfer process at the molecular level. From the RDF for the end atoms of the donor molecules with the COM of C$_{70}$ (Figure S7, Supporting Information), it is found that **DRCN7T** molecules have a closer contact with fullerene acceptors than **DERHD7T**, which should facilitate the intermolecular charge transfer from oligothiophene donors to fullerenes. Based on these results, we proposed a molecular picture for the efficient charge transfer process in these oligothiophene derivative blended with PC$_{71}$BM. The HOMO electron densities are mainly delocalized on the sepithiophene backbone at the ground state, and transfer from the oligothiophene backbone to the electron-withdrawing groups after photoexcitation (the intramolecular charge transfer process). Then the efficient intermolecular charge transfer from oligothiophene donors to PC$_{71}$BM can occur directly if the end groups and PC$_{71}$BM have closer contacts. This is quite similar to the working mechanisms for the electron transfer process from end groups of organic dyes to TiO$_2$ in dye-sensitized solar cells (DSSCs).[44–46] Recent time-resolved ultrafast pump–probe experiments have also proved that one of the important distinctions in the donor–acceptor-type polymers is that the lowest energy excitonic transition exhibits the partial charge-transfer feature,[47] and these intramolecular charge transfer states can eventually facilitate the final charge separation at the donor:acceptor interfaces.[47,48]

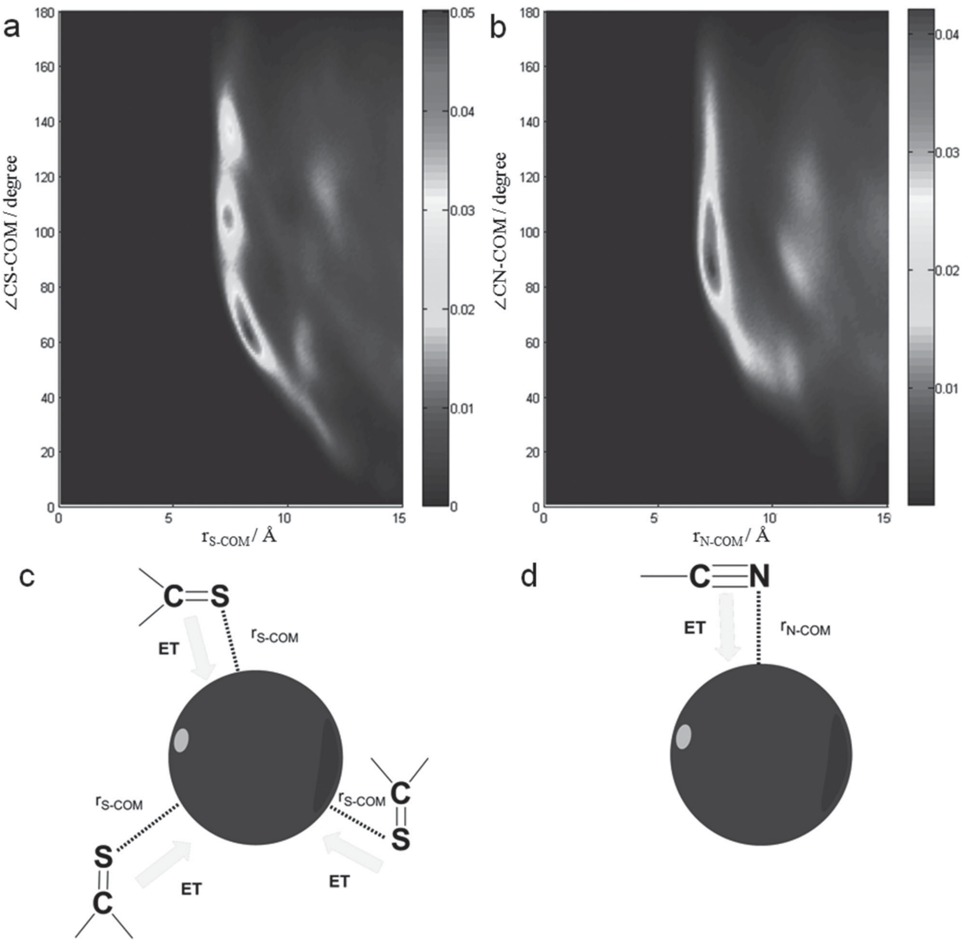

Figure 4. 2D distance-angle ($r_{\text{A-COM}}$, ∠CA-COM) distribution between the end atom and the COM of C_{70} in a) **DERHD7T**:$PC_{71}BM$ blend and b) **DRCN7T**:$PC_{71}BM$ blend. Cartoons illustrating different contacts for the end atoms of c) **DERHD7T** or d) **DRCN7T** with $PC_{71}BM$ (ET represents electron transfer).

Then orientation of the end groups with respect to $PC_{71}BM$ molecules was calculated according to the angle of end groups (C=S or C≡N)-COM of C_{70} (∠CA-COM, in which A refers to S or N atoms) and the distance between end atoms and COM of C_{70} ($r_{\text{A-COM}}$). As shown in **Figure 4**a,b, there are three peaks for the **DERHD7T**-based system, and only one major peak in **DRCN7T**:$PC_{71}BM$. For **DERHD7T**:$PC_{71}BM$, the end groups have three orientations with respect to C_{70}, whose angles are 65°, 105°, and 135°, respectively (Figure 4c). Meanwhile, the end groups of **DRCN7T** just have one major orientation with respect to C_{70} at 90° (Figure 4d). This observation is quite similar to the different adsorption structures of various dye anchor groups on TiO_2 in DSSC, which directly influences the charge transfer dynamics and device performance.[44–46] The electronic couplings (V_e) for electron transfer from oligothiophene donors to the fullerenes are then calculated at B3LYP/6-31G level (Table S3, Supporting Information), with average values of 8.23 and 11.34 meV for **DERHD7T**:$PC_{71}BM$ and **DRCN7T**:$PC_{71}BM$ systems, respectively. Thus, the charge transfer and the subsequent charge separation can occur more efficiently for the **DRCN7T**:$PC_{71}BM$ blend than **DERHD7T**:$PC_{71}BM$ according to Marcus electron transfer theory.[49–51] Based on these results, we conclude that **DRCN7T** packs regularly with $PC_{71}BM$, and $PC_{71}BM$ molecules also aggregate tightly at the interface, which facilitates electron delocalization and efficient charge separation.

The micromorphology of the intermixed regions for two important small molecular donors **DRCN7T** and **DERHD7T** blended with $PC_{71}BM$ were investigated by all-atom MD simulations. The fullerenes were found to aggregate more tightly in **DRCN7T**-based systems, and the DCM groups also exhibit regular contacts with $PC_{71}BM$, which facilitates the electron delocalization and efficient charge separation at the interfaces. This finding is in good agreement with our experimental 2D-GISAXS profile. This is the first time to investigate the fullerene aggregation with fully atomistic model using MD simulations, and the relationship between micromorphology and device performance obtained in this work provides a new insight for future design of high-performance donors.

Experimental Section

The MD simulations were carried out with the GROMACS program (version 4.5.5).[36–38] Both blend systems consist of 257 $PC_{71}BM$ molecules, while the number of **DERHD7T** and **DRCN7T** molecules are

332 and 320, respectively, consistent with the experimental mole ratio of donors and acceptors.[7] All the atoms, including hydrogen atoms, were treated explicitly in this detailed atomistic model. The OPLS-AA force field[52–57] is adopted to parameterize the molecular models, as listed in Figures S1 and S2, Tables S1–S10 (Supporting Information). The partial charges were derived by fitting our calculated ab initio electrostatic potential by Gaussian[58] with the restrained electrostatic potential (RESP) method.[59] The cutoff for the van der Waals and real-space electrostatic interactions were set to be 9 Å, and the particle mesh Ewald (PME) method[60] was used to treat the long-range electrostatic interaction in the reciprocal space. The initial configurations were first generated by putting the molecules in a large box with the periodical boundary condition applied, and then cooled from 400 K down to 300 K gradually. Both pure and blend systems were equilibrated in the isothermal–isobaric (*NPT*) ensemble, coupled to a Berendsen barostat at the pressure of 1 atm and a Berendsen thermostat at the temperature of 300 K. The production run lasted 100 ns after an equilibration run of 100 ns. All structural analyses were performed on the sampled configurations.

Supporting Information

Supporting Information is available from the Wiley Online Library or from the author.

Acknowledgements

G.L. and A.L. contributed equally to this work. The authors gratefully acknowledge financial support from the MOST (Grant Nos. 2014CB643502 and 2012CB933401), NSFC (Grant Nos. 91433101, 51422304, 21373118, 21421001, and 51373078), NSF of Tianjin City (Grant No. 13RCGFGX01121), and PCSIRT (IRT1257). The authors thank beamline BL16B1 (Shanghai Synchrotron Radiation Facility) for providing beam time. The MD simulations were performed on TianHe-1(A) at the National Supercomputer Center in Tianjin, China.

Received: July 11, 2015
Revised: August 1, 2015

---

[1] A. Mishra, P. Bäuerle, *Angew. Chem. Int. Ed.* **2012**, *51*, 2020.
[2] B. Walker, C. Kim, T. Q. Nguyen, *Chem. Mater.* **2011**, *23*, 470.
[3] Y. Lin, Y. Li, X. Zhan, *Chem. Soc. Rev.* **2012**, *41*, 4245.
[4] Y. Chen, X. Wan, G. Long, *Acc. Chem. Res.* **2013**, *46*, 2645.
[5] J. E. Coughlin, Z. B. Henson, G. C. Welch, G. C. Bazan, *Acc. Chem. Res.* **2013**, *47*, 257.
[6] a) V. Gupta, A. K. K. Kyaw, D. H. Wang, S. Chand, G. C. Bazan, A. J. Heeger, *Sci. Rep.* **2013**, *3*, 1965; b) K. K. Kyaw, D. H. Wang, V. Gupta, J. Zhang, S. Chand, G. C. Bazan, A. J. Heeger, *Adv. Mater.* **2013**, *25*, 2397; c) K. K. Kyaw, D. H. Wang, V. Gupta, W. L. Leong, L. Ke, G. C. Bazan, A. J. Heeger, *ACS Nano* **2013**, *7*, 4569; d) J. A. Love, I. Nagao, Y. Huang, M. Kuik, V. K. Gupta, C. J. Takacs, J. E. Coughlin, L. Qi, T. S. van der Poll, E. J. Kramer, A. J. Heeger, T. Q. Nguyen, G. C. Bazan, *J. Am. Chem. Soc.* **2014**, *136*, 5591.
[7] Q. Zhang, B. Kan, F. Liu, G. Long, X. Wan, X. Chen, Y. Zuo, W. Ni, H. Zhang, M. Li, Z. Hu, F. Huang, Y. Cao, Z. Liang, M. Zhang, P. R. Thomas, Y. Chen, *Nat. Photonics* **2015**, *9*, 35.
[8] B. Kan, Q. Zhang, M. Li, X. Wan, W. Ni, G. Long, Y. Wang, X. Yang, H. Feng, Y. Chen, *J. Am. Chem. Soc.* **2014**, *136*, 15529.
[9] Z. He, C. Zhong, S. Su, M. Xu, H. Wu, Y. Cao, *Nat. Photonics* **2012**, *6*, 593.
[10] S. H. Liao, H. J. Jhuo, Y. S. Cheng, S. A. Chen, *Adv. Mater.* **2013**, *25*, 4766.
[11] G. Long, X. Wan, B. Kan, Y. Liu, G. He, Z. Li, Y. Zhang, Y. Zhang, Q. Zhang, M. Zhang, Y. Chen, *Adv. Energy Mater.* **2013**, *3*, 639.
[12] J. Zhou, Y. Zuo, X. Wan, G. Long, Q. Zhang, W. Ni, Y. Liu, Z. Li, G. He, C. Li, B. Kan, M. Li, Y. Chen, *J. Am. Chem. Soc.* **2013**, *135*, 8484.
[13] G. Long, X. Wan, B. Kan, Z. Hu, X. Yang, Y. Zhang, M. Zhang, H. Wu, F. Huang, S. Su, Y. Cao, Y. Chen, *ChemSusChem* **2014**, *7*, 2358.
[14] Z. Li, G. R. He, X. J. Wan, Y. S. Liu, J. Y. Zhou, G. K. Long, Y. Zuo, M. T. Zhang, Y. S. Chen, *Adv. Energy Mater.* **2012**, *2*, 74.
[15] J. M. Szarko, B. S. Rolczynski, S. J. Lou, T. Xu, J. Strzalka, T. J. Marks, L. Yu, L. X. Chen, *Adv. Funct. Mater.* **2014**, *24*, 10.
[16] W. Li, K. H. Hendriks, A. Furlan, W. S. C. Roelofs, M. M. Wienk, R. A. J. Janssen, *J. Am. Chem. Soc.* **2013**, *135*, 18942.
[17] G. D'Avino, L. Muccioli, C. Zannoni, *Adv. Funct. Mater.* **2015**, *25*, 1985.
[18] W. Shin, T. Yasuda, Y. Hidaka, G. Watanabe, R. Arai, K. Nasu, T. Yamaguchi, W. Murakami, K. Makita, C. Adachi, *Adv. Energy Mater.* **2014**, *4*, 1400879.
[19] T. T. To, S. Adams, *Phys. Chem. Chem. Phys.* **2014**, *16*, 4653.
[20] Y. T. Fu, D. A. da Silva Filho, G. Sini, A. M. Asiri, S. G. Aziz, C. Risko, J. L. Brédas, *Adv. Funct. Mater.* **2014**, *24*, 3790.
[21] S. Y. Reddy, V. K. Kuppa, *J. Phys. Chem. C* **2012**, *116*, 14873.
[22] E. Jankowski, H. S. Marsh, A. Jayaraman, *Macromolecules* **2013**, *46*, 5775.
[23] C. K. Lee, C. W. Pao, *J. Phys. Chem. C* **2014**, *118*, 11224.
[24] L. Meng, Y. Shang, Q. Li, Y. Li, X. Zhan, Z. Shuai, R. G. E. Kimber, A. B. Walker, *J. Phys. Chem. B* **2009**, *114*, 36.
[25] C. Groves, N. Greenham, *Top. Curr. Chem.* **2014**, *352*, 257.
[26] P. K. Watkins, A. B. Walker, G. L. B. Verschoor, *Nano Lett.* **2005**, *5*, 1814.
[27] D. Chandler, *Nature* **2005**, *437*, 640.
[28] F. C. Jamieson, E. B. Domingo, T. Carthy-Ward, M. Heeney, N. Stingelin, J. R. Durrant, *Chem. Sci.* **2012**, *3*, 485.
[29] S. Shoaee, S. Subramaniyan, H. Xin, C. Keiderling, P. S. Tuladhar, F. Jamieson, S. A. Jenekhe, J. R. Durrant, *Adv. Funct. Mater.* **2013**, *23*, 3286.
[30] G. Lakhwani, A. Rao, R. H. Friend, *Annu. Rev. Phys. Chem.* **2014**, *65*, 557.
[31] S. Gélinas, A. Rao, A. Kumar, S. L. Smith, A. W. Chin, J. Clark, T. S. van der Poll, G. C. Bazan, R. H. Friend, *Science* **2014**, *343*, 512.
[32] J. L. Brédas, *Science* **2014**, *343*, 492.
[33] A. Rao, P. C. Y. Chow, S. Gelinas, C. W. Schlenker, C. Z. Li, H. L. Yip, A. K. Y. Jen, D. S. Ginger, R. H. Friend, *Nature* **2013**, *500*, 435.
[34] B. M. Savoie, A. Rao, A. A. Bakulin, S. Gelinas, B. Movaghar, R. H. Friend, T. J. Marks, M. A. Ratner, *J. Am. Chem. Soc.* **2014**, *136*, 2876.
[35] F. Gao, O. Inganas, *Phys. Chem. Chem. Phys.* **2014**, *16*, 20291.
[36] D. Van Der Spoel, E. Lindahl, B. Hess, G. Groenhof, A. E. Mark, H. J. C. Berendsen, *J. Comput. Chem.* **2005**, *26*, 1701.
[37] B. Hess, C. Kutzner, D. van der Spoel, E. Lindahl, *J. Chem. Theory Comput.* **2008**, *4*, 435.
[38] H. J. C. Berendsen, D. van der Spoel, R. van Drunen, *Comput. Phys. Commun.* **1995**, *91*, 43.
[39] H. V. R. Annapureddy, H. K. Kashyap, P. M. De Biase, C. J. Margulis, *J. Phys. Chem. B* **2010**, *114*, 16838.
[40] T. Yan, Y. Wang, C. Knox, *J. Phys. Chem. B* **2010**, *114*, 6905.
[41] W. R. Wu, U. S. Jeng, C. J. Su, K. H. Wei, M. S. Su, M. Y. Chiu, C. Y. Chen, W. B. Su, C. H. Su, A. C. Su, *ACS Nano* **2011**, *5*, 6233.
[42] P. Müller-Buschbaum, *Adv. Mater.* **2014**, *26*, 7692.
[43] E. Y. Sheu, *Phys. Rev. A* **1992**, *45*, 2428.
[44] A. Hagfeldt, M. Grätzel, *Acc. Chem. Res.* **2000**, *33*, 269.

[45] T. Moehl, H. N. Tsao, K. L. Wu, H. C. Hsu, Y. Chi, E. Ronca, F. De Angelis, M. K. Nazeeruddin, M. Grätzel, *Chem. Mater.* **2013**, *25*, 4497.

[46] S. Ye, A. Kathiravan, H. Hayashi, Y. Tong, Y. Infahsaeng, P. Chabera, T. Pascher, A. P. Yartsev, S. Isoda, H. Imahori, V. Sundström, *J. Phys. Chem. C* **2013**, *117*, 6066.

[47] B. Carsten, J. M. Szarko, H. J. Son, W. Wang, L. Lu, F. He, B. S. Rolczynski, S. J. Lou, L. X. Chen, L. Yu, *J. Am. Chem. Soc.* **2011**, *133*, 20468.

[48] Z. Guo, D. Lee, R. D. Schaller, X. Zuo, B. Lee, T. Luo, H. Gao, L. Huang, *J. Am. Chem. Soc.* **2014**, *136*, 10024.

[49] R. A. Marcus, *Rev. Mod. Phys.* **1993**, *65*, 599.

[50] J. L. Brédas, D. Beljonne, V. Coropceanu, J. Cornil, *Chem. Rev.* **2004**, *104*, 4971.

[51] L. Wang, G. Nan, X. Yang, Q. Peng, Q. Li, Z. Shuai, *Chem. Soc. Rev.* **2010**, *39*, 423.

[52] W. L. Jorgensen, D. S. Maxwell, J. Tirado-Rives, *J. Am. Chem. Soc.* **1996**, *118*, 11225.

[53] D. L. Cheung, A. Troisi, *J. Phys. Chem. C* **2010**, *114*, 20479.

[54] K. Do, D. M. Huang, R. Faller, A. J. Moule, *Phys. Chem. Chem. Phys.* **2010**, *12*, 14735.

[55] W. D. Cornell, P. Cieplak, C. I. Bayly, I. R. Gould, K. M. Merz, D. M. Ferguson, D. C. Spellmeyer, T. Fox, J. W. Caldwell, P. A. Kollman, *J. Am. Chem. Soc.* **1995**, *117*, 5179.

[56] M. K. Dahlgren, P. Schyman, J. Tirado-Rives, W. L. Jorgensen, *J. Chem. Inf. Model.* **2013**, *53*, 1191.

[57] J. N. C. Lopes, A. L. A. H. Pádua, *J. Phys. Chem. B* **2006**, *110*, 19586.

[58] M. J. Frisch, G. W. Trucks, H. B. Schlegel, G. E. Scuseria, M. A. Robb, J. R. Cheeseman, G. Scalmani, V. Barone, B. Mennucci, G. A. Petersson, H. Nakatsuji, M. Caricato, X. Li, H. P. Hratchian, A. F. Izmaylov, J. Bloino, G. Zheng, J. L. Sonnenberg, M. Hada, M. Ehara, K. Toyota, R. Fukuda, J. Hasegawa, M. Ishida, T. Nakajima, Y. Honda, O. Kitao, H. Nakai, T. Vreven, J. A. Montgomery Jr., J. E. Peralta, F. Ogliaro, M. Bearpark, J. J. Heyd, E. Brothers, K. N. Kudin, V. N. Staroverov, R. Kobayashi, J. Normand, K. Raghavachari, A. Rendell, J. C. Burant, S. S. Iyengar, J. Tomasi, M. Cossi, N. Rega, J. M. Millam, M. Klene, J. E. Knox, J. B. Cross, V. Bakken, C. Adamo, J. Jaramillo, R. Gomperts, R. E. Stratmann, O. Yazyev, A. J. Austin, R. Cammi, C. Pomelli, J. W. Ochterski, R. L. Martin, K. Morokuma, V. G. Zakrzewski, G. A. Voth, P. Salvador, J. J. Dannenberg, S. Dapprich, A. D. Daniels, Ö. Farkas, J. B. Foresman, J. V. Ortiz, J. Cioslowski, D. J. Fox, *Gaussian 09*, Revision B.01, Gaussian, Inc., Wallingford, CT **2010**.

[59] T. Fox, P. A. Kollman, *J. Phys. Chem. B* **1998**, *102*, 8070.

[60] U. Essmann, L. Perera, M. L. Berkowitz, T. Darden, H. Lee, L. G. Pedersen, *J. Chem. Phys.* **1995**, *103*, 8577.